phys. stat. sol. (a) **188**, No. 4, 1233–1242 (2001)

Theory for Modeling the Optical Properties of Surfaces

G. Onida[1]) (a), W. G. Schmidt (b), O. Pulci (a), M. Palummo (a), A. Marini (a), C. Hogan (a), and R. Del Sole (a)

(a) Istituto Nazionale per la Fisica della Materia e Dipartimento di Fisica dell'Università di Roma "Tor Vergata", Via della Ricerca Scientifica, I-00133 Roma, Italy

(b) Institut für Festkörpertheorie und Theoretische Optik, Friedrich-Schiller-Universität, Max-Wien-Platz 1, D-07743 Jena, Germany

(Received August 10, 2001; in revised form August 17, 2001; accepted August 23, 2001)

Subject classification: 73.20.At; 78.20.Bh; 78.68.+m; S1.3; S5.11; S5.12; S7.12

We summarize the theoretical framework and some of the computational methods currently used for the calculation of the optical properties of surfaces within the "ab initio" scheme. Applications and examples are given for calculations including self-energy, excitonic, and local-field effects, with an emphasis on convergence problems and on the approximations related to the pseudopotential approach.

1. Introduction

When studying the optical properties of surfaces one is faced with two major difficulties. First of all, one must deal with the fact that real surfaces are *per se* complex physical systems: in general, the ground state geometry (atomic positions) is unknown, and, unlike in bulk crystals, can involve many degrees of freedom. Secondly, one must adequately describe the interaction of the surface with the light. On one level, this problem has been solved: all the details of the interaction can in theory be encompassed in a dielectric tensor formalism (see, for example, [1]). However, relating this formalism to the quantum mechanical response of the surface involves another level of complexity, due to the fact that optical properties always involve excited states of the system. Indeed, a thorough computational description of this process remains very difficult to achieve even for the simplest, elemental bulk semiconductors. For these reasons, calculations are usually performed at different levels of sophistication, involving various simplifications and approximations, according to the accuracy required and the numerical heaviness of the calculations themselves. In the following, we will focus on the latter point, and in particular discuss state-of-the-art *ab-initio* techniques which enable the inclusion of self-energy, excitonic, and local-field effects in the optical response function. We will also illustrate some problems arising from the use of (norm-conserving) pseudopotentials, i.e. the effect of nonlocality therein, and the role of the "core" region in the calculation of dipole transition matrix elements. Parameterized methods, such as the semi-empirical tight-binding scheme, will not be considered here. To illustrate the successes and limitations of the methods and approximations used, we present some examples related to Ge and GaAs surfaces.

[1]) Corresponding author; Phone: +39.06.72594501; Fax: +39.06.2023507; e-mail: onida@roma2.infn.it

 0031-8965/01/18812-1233 $ 17.50+.50/0

2. Theoretical Framework

Ab-initio calculations of optical properties are most conveniently performed according to the independent quasiparticle (IQP) picture, or equivalently, at the RPA (random-phase-approximation) level. In this scheme, the imaginary part of the dielectric function (or in realistic surface calculations, the half-slab polarizability) is computed by simply summing over independent contributions coming from the valence–conduction band pairs at the different k points of the Brillouin zone. Given the quasiparticle energies $E_{k,n}$ and wavefunctions ϕ_n, the standard expression for the half-slab polarizability $\alpha_{ii}^{\mathrm{hs}}(\omega)$, written in terms of the momentum matrix elements representing vertical transition probabilities between valence and conduction states, is given as

$$\alpha_{ii}^{\mathrm{hs}}(\omega) = \frac{\pi e^2}{m\omega^2 A d} \sum_{k,v,c} |\langle \phi_{\mathrm{v}} | \, p_i \, | \phi_{\mathrm{c}} \rangle|^2 \, \delta(E_{k,\mathrm{c}} - E_{k,\mathrm{v}} - \hbar\omega) \,, \tag{1}$$

where i denotes the direction of the incident light polarization in the surface plane, d is the slab thickness, $\mathbf{p}$ is the momentum, A is the area of the surface unit cell and m the electronic mass. Expression (1) can be derived from a polarization function P_{IQP} defined as $G_0 G_0$, the product of two one-particle Green's functions, and thus is consistent with the IQP approximation. The dynamical polarizability $\alpha_{ii}^{\mathrm{hs}}(\omega)$ may be formally related to experimentally observed quantities, such as the normal incidence reflectance R, or the Reflectance Anisotropy Spectra (RAS), defined by $(R_x - R_y)/R$. Use is then made of the relation [1]

$$\frac{R_i - R_0}{R_0} = \frac{4\omega}{c} \, \mathrm{Im} \, \frac{4\pi d \alpha_{ii}^{\mathrm{hs}}(\omega)}{\epsilon_{\mathrm{bulk}}(\omega) - 1} \,, \tag{2}$$

where R_0 is the Fresnel reflectivity, and ϵ_{bulk} the (complex) bulk dielectric function. The critical quantities here are the excited state energies $E_{k,n}$ and wavefunctions ϕ_n, which are usually taken from the ground-state calculation of the system within the Density Functional Theory (DFT). The DFT results – i.e., the one-particle (Kohn-Sham) eigenvalues and eigenfunctions – can in fact be used as a starting point for the excited-state calculations. Moreover, within DFT efficient algorithms such as the Car-Parrinello method [2] can be used to search for the equilibrium geometry of relaxed or reconstructed surfaces, possibly also in the presence of adsorbates. However, it is well known that Kohn-Sham (KS) eigenvalues appear in the DFT only as Lagrange multipliers to ensure the ortho-normality of the wavefunctions in the minimization of the energy functional: they (in contrast to Hartree-Fock) cannot be directly identified with electron addition or removal energies, since DFT does not possess an equivalent of Koopman's theorem. Instead, the electronic band structure should be obtained rigorously within many-body perturbation theory, where excitation energies are given by the poles of the Green's functions. When only one-particle excitations are required, such as those involved in photoemission (PE) or inverse photoemission (IPE) experiments, one-particle Green's functions need to be used. They can be obtained through the electron self-energy Σ, usually approximated according to the so-called GW approach. The GW approach is based on an expansion of Σ in terms of the dynamically screened Coulomb interaction W, and was derived by Hedin in 1965 [3]. In optical absorption processes, however, it is necessary to go beyond this one-quasiparticle level. In fact, the energy of the absorbed photon can differ from the bare (algebraic) sum of the hole and electron energies: it is

often necessary to take into account the electron–hole interaction. The latter can produce not only absorption below the gap, due to bound exciton states, but also can induce appreciable distortions on the line shape above the continuous absorption edge. The calculation of excitonic effects from first-principles through the solution of the Bethe-Salpeter equation (BSE) for the two-particle Green's function is only a recent achievement [4], and until now, has been seldom applied to real surfaces.

2.1 Self-energy effects

To understand how one- and two-particle Green's functions can be computed starting from a ground-state DFT calculation (usually performed within the Local Density Approximation (LDA) or the Generalized Gradient Approximation (GGA)) one has to consider the relation between Kohn-Sham eigenvalues, the poles of the one-particle Green's function G, and the experimental band energies, i.e., those measured in photoemission (PE) or inverse photoemission (IPE). The latter should be compared with the poles of the one-particle G, that can be formally expanded as [5]

$$G(\mathbf{r},\mathbf{r}';\omega) = \sum_{\lambda} \frac{\psi_\lambda(\mathbf{r},\omega)\,\psi_\lambda^*(\mathbf{r}',\omega)}{\omega - E_\lambda(\omega)}\,, \tag{3}$$

with $\psi_\lambda(\mathbf{r},\omega)$ solutions of

$$[-\tfrac{1}{2}\,\nabla^2 + V_{\text{ext}} + V_{\text{Hartree}}]\,\psi_\lambda(\mathbf{r},\omega) + \int \mathrm{d}\mathbf{r}'\,\Sigma(\mathbf{r},\mathbf{r}',\omega)\,\psi_\lambda(\mathbf{r}',\omega) = E_\lambda(\omega)\,\psi_\lambda(\mathbf{r},\omega)\,. \tag{4}$$

G is hence determined by the non-local, non-hermitian and frequency dependent self-energy operator Σ, and its poles can be well approximated by the quasi-particle (QP) energies $\epsilon_\lambda^{\text{QP}}$ solution of $\epsilon_\lambda^{\text{QP}} = E_\lambda(\omega)|_{\omega=\epsilon_\lambda^{\text{QP}}}$. Equation (4) is formally similar to the Kohn-Sham equations which are solved in the determination of the ground-state properties, where the local end energy independent exchange-correlation potential $V_{\text{xc}}(\mathbf{r})$ has been substituted by Σ. Hence, KS eigenvalues can be considered as a zeroth-order approximation to the true QP energies, if the exchange-correlation (xc) potential of the DFT is interpreted as an approximation to the true self-energy operator Σ. This suggests the possibility of a first-order, perturbative solution of Eq. (4) with respect to $\left(\Sigma - V_{\text{xc}}^{\text{LDA}}\right)$, where $V_{\text{xc}}^{\text{LDA}}$ is the xc potential of the LDA. The diagonal matrix elements of $\left(\Sigma - V_{\text{xc}}^{\text{LDA}}\right)$ then give the QP energies as

$$\epsilon_{nk}^{\text{LDA}} + \langle\phi_{nk}^{\text{LDA}}|\,\Sigma(\epsilon_{nk}^{\text{QP}}) - V_{\text{xc}}^{\text{LDA}}\,|\phi_{nk}^{\text{LDA}}\rangle - \epsilon_{nk}^{\text{QP}} = 0\,. \tag{5}$$

Due to the frequency dependence of $\langle\Sigma(\omega)\rangle$, the determination of the QP energies $\epsilon_{nk}^{\text{QP}}$ starting from the DFT-LDA values $\epsilon_{nk}^{\text{LDA}}$ requires either a linearization of the energy-dependence of Σ, or the use of an iterative procedure [6]. The resulting corrections to the KS eigenvalues are called self-energy corrections to the Kohn-Sham eigenvalues, and must in principle be obtained for every state and every k point needed. The quasi-particle also acquires a width, given by the imaginary part of $\Sigma(\epsilon_{nk}^{\text{QP}})$, that increases going towards higher binding energies. This width determines the lifetime of the related excited state (QP lifetime). The application of this method to semiconductors, insulators, surfaces and atomic clusters generally yields energy levels in good agreement with experiments [7]. The gaps between filled and empty states, underestimated within DFT,

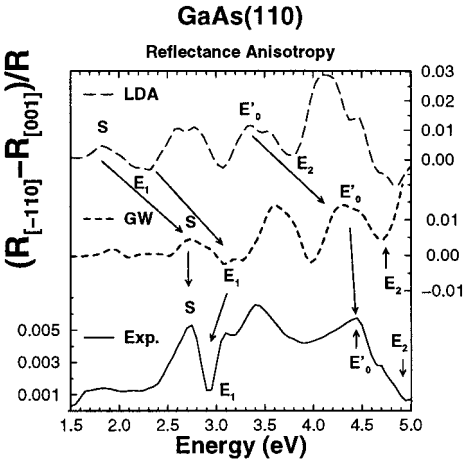

Fig. 1. Reflectance anisotropy spectrum of GaAs(110) computed at the LDA level (top) and including *GW* self-energy corrections to the KS eigenvalues (middle), from [8]. Bottom: experimental data from [9]

often increase by an almost constant amount, suggesting the use of a scissors operator: this consists of a rigid upward shift of the LDA conduction bands, in order to mimic the effects of $(\Sigma - V_{\mathrm{xc}}^{\mathrm{LDA}})$, thereby avoiding the explicit calculation of self-energy corrections over many k points and bands. This approach has been widely and successfully used for many bulk semiconductors. However, in the case of surfaces the validity of the scissors operator can be questioned, since self-energy corrections can be different for surface and bulk states, which experience a different screening. For example, a situation of this kind has been found in *GW* calculations for the valence bands of GaAs(110) [8]. In that specific case, a simplification was possible based on the finding of an almost linear relation between self-energy corrections and surface localization of the states. This allows for the restriction of the calculation of the true *GW* corrections to a small set of bands and k points. The resulting shifts can then be extrapolated to a larger set of states (all the LDA bands and k points), based only on the knowledge of their surface localization. The resulting RAS spectrum from Ref. [8] is reproduced in Fig. 1. Disappointingly, the comparison with the experimental data shows only a qualitative agreement.

In fact, this is a quite typical situation: calculations including self-energy effects in the band structure energies usually agree well with photoemission and inverse photoemission data, but when the theoretical optical spectra are compared with measured data, the agreement is often unsatisfactory. This is mainly due to the neglection of excitonic effects, as mentioned above.

2.2 Excitonic and local-field effects

Even for bulk semiconductors, a quantitative agreement between theory and experiment for optical absorption spectra can only be achieved by including electron–hole interaction effects in the calculation. The most striking and clear example is given by bulk silicon (Fig. 2), where excitons have been shown to induce a strong enhancement of the E_1 peak [4, 10]. Furthermore, the e–h interaction may also induce a redshift of the spectral peaks, which partially cancels the blueshift arising from the self-energy corrections. The RPA spectrum calculated with the LDA energy bands is redshifted, with respect to the experimental results [11], by about 0.5 eV. This is due to the usual underestimation of the transitions energies, typical of DFT calculations. The RPA spectrum obtained with the *GW* energy bands becomes blueshifted with respect to the experimental data, and the sizeable discrepancies in the lineshape, already present in the

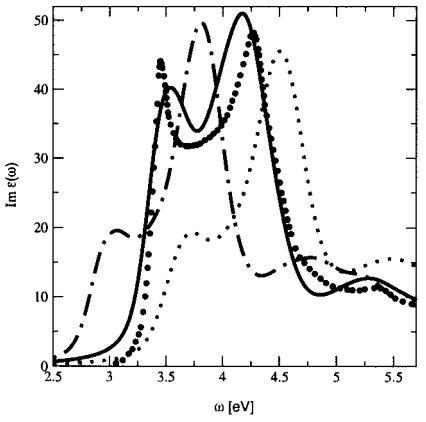

Fig. 2. Silicon absorption spectrum. Big dots: experiment [11]; dash-dotted curve: LDA with LFE; small dots: *GW* result; full line: including excitonic effects

LDA spectrum, remain uncorrected (especially at the E_1 peak). Finally, when including GW energies *and* excitonic effects, a quantitative agreement with the experimental spectrum is found. In particular, the inclusion of excitonic effects enhances the E_1 peak by almost 100%. The local-field effects can in principle be included straightforwardly by adopting the correct definition of the macroscopic dielectric function ϵ_{M}, i.e. by taking the inverse of the average of the inverse dielectric function (and similarly for the macroscopic half-slab polarizability). The latter can be obtained either by inverting the full ϵ matrix, or by computing directly ϵ^{-1} as $1 + v\chi$, where v is the Coulomb potential and χ is obtained from P_{IQP} with a Dyson-like equation

$$\chi = P_{\mathrm{IQP}} + P_{\mathrm{IQP}} v \chi \,. \tag{6}$$

However, it is also possible to obtain the macroscopic dielectric function ϵ_{M} (including LFE) directly from a polarization function $\bar{P}$ such that $\epsilon_{\mathrm{M}} = 1 - v\bar{P}$. In this way, $\bar{P}$ must obey an expression similar to Eq. (6), but where v is substituted by $\bar{v}$, the Coulomb potential without its long-range ($G = 0$) Fourier component [12]. This formulation is useful because it allows one to put LFE and e–h interaction effects on the same footing, and to obtain them both within a single calculation. In fact, it is precisely by substituting $P_{\mathrm{IQP}} = G_0 G_0$ with a more general P that one can include the excitonic effects in the calculation of ϵ. The expression for this more general P can be derived from Hedin's equations [3]:

$$\Sigma(12) = i \int G(13)\, \Gamma(324)\, W(41)\, \mathrm{d}(34)\,, \tag{7}$$

$$W(12) = v(12) + \int v(13)\, P(34)\, W(42)\, \mathrm{d}(34)\,, \tag{8}$$

$$P(12) = -i \int G(13)\, G(41)\, \Gamma(342)\, \mathrm{d}(34)\,, \tag{9}$$

$$\Gamma(123) = \delta(12)\, \delta(13) + \int \frac{\delta \Sigma(12)}{\delta G(45)}\, G(46)\, G(75)\, \Gamma(673)\, \mathrm{d}(4567) \tag{10}$$

by considering in Eq. (9) a vertex function Γ different from unity and by multiplying Eq. (10) with $G_0 G_0$ on the left. In this way, one can define a polarizability P which contains at the same time both the LFE and the e–h interaction. The equation for P is still Dyson-like, and reads

$$P = G_0 G_0 + G_0 G_0 K P \,. \tag{11}$$

Equation (11) is known as the Bethe-Salpeter equation (BSE). Its kernel K contains two terms: the first is $\bar{v}$, which yields the LFE; the second term is $\delta\Sigma/\delta G$, which in the *GW* approximation for Σ, and neglecting $\delta W/\delta G$, turns out to be the screened Coulomb interaction W. The "price" to be paid from the numerical point of view is repre-

sented by the necessity of diagonalizing an $(N_k N_v N_c \times N_k N_v N_c)$ matrix, where N_k, N_v, and N_c, are the number of k points, valence bands, and conduction bands, respectively. In particular for large systems, characterized by many electron–hole pair interactions, iterative schemes based on the reformulation of the eigenvalue problem as an initial-value problem may help to overcome the computational difficulties [13].

2.3 Illustrative examples

The methods described above for the calculation of the macroscopic dielectric function including excitonic and local-field effects, implemented in the ab-initio plane-wave scheme, have led to a quantitative description of the absorption spectra of many systems. The first applications were to small clusters [14] and to bulk semiconductors; in the last two years, however, applications to real surfaces started to appear [13, 15, 16]. The case of Ge(111)(2×1) is particularly interesting, since it is a surface which can exist in two different isomeric forms: one is the standard Pandey reconstruction, with buckled chains on the topmost layer; the other is an equivalent Pandey reconstruction, but where the chains undergo a negative buckling [16]. DFT-LDA ground-state calculations for the two isomers have shown them to be almost degenerate in energy. Hence, the uncertainties of the calculations (mainly due to the approximated form of the exchange-correlation potential), make it impossible, based only on total energy results, to predict the most stable form. Excited state calculations, instead, allow us to make a clearer distinction between the positively and negatively buckled surfaces. In fact, the main surface peak in the Reflectance Difference Spectra (RDS) is due to transitions involving essentially a single pair of flat surface bands, localized on the topmost layer. This peak appears to be redshifted by about 0.2 eV in the case of the negatively buckled chains, with respect to the standard Pandey geometry. The important point is that for a comparison of the calculated spectra with the experiments to be useful, i.e. to discriminate between the two isomers, it is necessary to know the *absolute* energy position of the theoretical peaks. This is possible if both self-energy corrections and excitonic effects are taken into account explicitly, avoiding a "scissors operator" method. The results (Fig. 3) strongly suggest the negatively buckled isomer as the dominant reconstruction of the measured sample. The existence of boundaries between positively and negatively buckled domains has also been proven experimentally by STM experiments [17]. A recent work has confirmed the prevalence of negatively buckled chains [18]. However, Si(111)(2×1) and Ge(111)(2×1) are quite unique cases, since only one pair of flat bands contribute to the surface

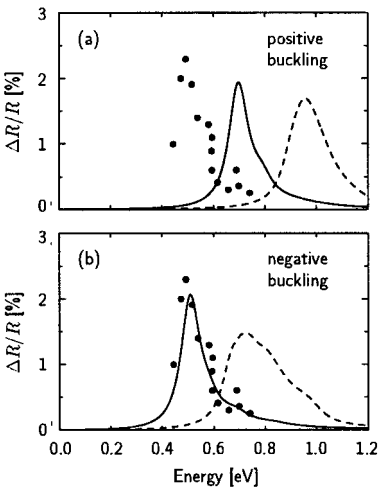

Fig. 3. Differential reflectivity spectrum of the Ge(111)(2×1) surface, from [16]. Dashed curve: *GW* calculation; full line: including excitonic effects; dots: experimental data from [19]

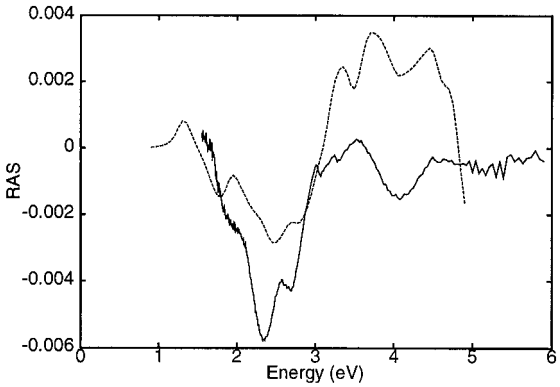

Fig. 4. RAS for the GaAs(100) $\zeta(4 \times 2)$ reconstructed surface. Dashed line: theoretical results computed within DFT-LDA + rigid shift towards the higher energies; full line: experimental results [24]. The shift included in the theoretical spectrum is 0.4 eV, and is meant to account for both self-energy and excitonic effects

optical peak. This allows one to reach the numerical convergence with a small number of k points. The computations get extremely expensive if both bulk and surface states at many k points need to be considered. In this case the the solution of the BSE requires approximations for the screening together with iterative schemes even for relatively simple surfaces such as Si(110):H [13]. For the large majority of real, reconstructed surfaces, possibly even with defects, full ab-initio self-energy + exciton calculations are still beyond computational reach. In those cases, it is hence necessary to stop the calculations at a lower level of sophistication. One possibility is the combination of DFT-LDA calculations with either a simple approximative approach to a full *GW* calculation [20] or the adoption of the scissors operator formalism. The latter approach is often completely sufficient in providing useful physical information, even if the exact amount of the required shift is sometimes lacking a rigorous theoretical derivation. The shift is in fact meant to mimic both the effects of self-energy and excitonic effects on the peak positions. It can, e.g., be taken from GW + exciton calculations for the bulk. However, it can as well be determined empirically, by a best fit to the experimentally measured surface optical spectra. The DFT-LDA + scissor approach has been successfully used in many cases, as, e.g., in the study of the optical properties of the (100) surfaces of Si [21, 22] and SiC [23]. We report here, as a novel example, results obtained for the GaAs(100) $\zeta(4 \times 2)$ surface (Fig. 4). Even if the agreement with the experiment remains qualitative, all the major spectral structures seem to be reproduced by the calculations.

2.4 Numerical convergence

The Brillouin zone integration is by far the most difficult convergence issue one has to tackle when calculating surface optical properties. Convergence tests for the RA of InP(110) have been performed [25] using several meshes of k points and different integration schemes. In Ref. [26] the RA of GaAs(110) has been calculated within the Tight Binding approach with 256, 1024 and 4096 special k points in the irreducible part of the surface BZ; the curves corresponding to the first two cases are clearly distinct from each other. The calculation with 4096 k points, instead, is almost coincident with that with 1024 k points. This means that 1024 k points are needed to achieve full quantitative convergence of the GaAs(110) RA. In the case of bulk Si and GaAs it turns out that, if a small broadening (less than 50 meV) is used, then thousands of k points

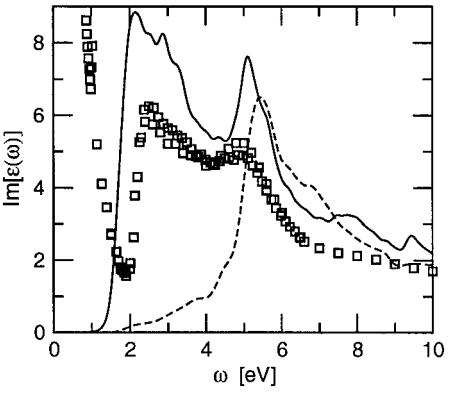

Fig. 5. Imaginary part of the macroscopic dielectric function of bulk copper with the use of the momentum operator (dashed line) or the velocity operator (full line) in Eq. (1). Squares represent the experimental data from [27]

(in the whole BZ) are needed to achieve full convergence of the spectrum. We found, however, that the use of random points, or at least a grid shifted off the high symmetry directions, is efficient in avoiding the overestimation of the spectral structures when only relatively few k points are used. Other convergence parameters are the number of atomic layers included in the slab used to simulate the surface, the amount of empty space separating the repeated slabs, and finally the kinetic energy cutoff in the plane-waves expansion of the one-particle states. All those parameters are usually easier to converge than the Brillouin zone sampling. Normally, a slab containing 10 to 20 atomic layers and with an inter-slab separation equivalent to about five layers is sufficient to obtain theoretical spectra which are converged within a few percent.

2.5 Influence of pseudopotential

Further technical problems arise in the calculation of optical properties due to the nonlocality of the (pseudo)potential (PP) used to generate the one-particle states. In this case the expression for the polarizability (Eq. (1)) is not strictly correct. Fortunately, the problem can be quite easily overcome by substituting the momentum operator with the velocity operator, which corresponds to considering the commutator of the nonlocal potential with the position operator. This point is not irrelevant: the fact that its effects on the optical properties of simple semiconductors such as Si and GaAs are small (and thus generally ignored in the calculation of their surface properties) cannot be generalized. As a counter-example, we show in Fig. 5 calculations for bulk copper, which has an extremely non-local pseudopotential. Using Eq. (1), one gets a completely wrong spectrum, with all the transitions below 4 eV almost totally suppressed. A further problem is represented by the contributions of the core region itself, where the pseudo-wavefunction is by definition different from the true all-electron wavefunction. Although it is difficult to draw any general conclusion about the size of these contributions to the optical matrix elements, in the case of bulk copper they turned out to be negligible, once the PP nonlocality has been correctly included in the calculation [28].

3. Summary and Conclusions

In conclusion, state-of-the-art ab-initio calculations of the optical properties of surfaces are rapidly evolving towards the same level of accuracy as already reached for bulk calculations, where it is nowadays possible to account for self-energy, excitonic and local-field effects, thus obtaining a quantitative description of the experimental absorption spectra. However, the use of the highest level of sophistication is only justified if one

can work at full numerical convergence. Particularly, in the case of optical spectra the convergence with respect to the Brillouin zone sampling is the most critical one. Convergence with respect to the slab thickness and to the number of plane waves is, on the other hand, easier to achieve. When the full convergence of the complete calculations cannot be reached, due to the limitations in computer power, simplified approaches may be extremely helpful. This holds in particular if one is mainly interested in qualitative features. A good compromise is often represented by LDA calculations + scissors operator, where both self-energy and excitonic effects are roughly taken into account by a rigid shift of the LDA spectrum. As a possible future alternative, Time-Dependent Density Functional (TDDFT) calculations should be mentioned. The TDDFT approach is promising since it is numerically much less demanding than the BSE approach. Unfortunately, the simple (static) LDA kernel, when used within TDDFT, fails to describe correctly the excitonic effects in solids. A better approximation for the TDDFT kernel is needed.

Acknowledgements This work has been supported by the INFM PRA project "1MESS" and by the EU through the NANOPHASE Research Training Network (Contract No. HPRN-CT-2000-00167). We thank L. Reining and V. Olevano for useful discussions. We are grateful to D. Paget for providing us the RAS experimental data on GaAs(100) prior to publication, and to S. Goedecker for providing us with an efficient code for Fast Fourier Transforms [29]. We acknowledge INFM for supercomputer resources under the Parallel Computing Initiative.

References

[1] R. Del Sole, Reflectance Spectroscopy – Theory, in: Photonic Probes of Surfaces, Ed. P. Halevi, Elsevier, Amsterdam 1995 (p. 131).
[2] R. Car and M. Parrinello, Phys. Rev. Lett. **55**, 2471 (1985).
[3] L. Hedin, Phys. Rev. **139**, A796 (1965).
[4] S. Albrecht, L. Reining, R. Del Sole, and G. Onida, Phys. Rev. Lett. **80**, 4510 (1998).
[5] P. M. Morse and H. Feshbach, Methods of Theoretical Physics, McGraw-Hill, New York 1953 (pp. 864–866).
[6] M. S. Hybertsen and S. G. Louie, Phys. Rev. Lett. **55**, 1418 (1985);
Phys. Rev. B **34**, 5390 (1986).
R. W. Godby, M. Schlüter, and L. J. Sham, Phys. Rev. Lett. **56**, 2415 (1986);
Phys. Rev. B **37**, 1059 (1988).
R. W. Godby and R. J. Needs, Phys. Rev. Lett. **62**, 1169 (1989).
[7] F. Aryasetiawan and O. Gunnarsson, Phys. Rev. Lett. **74**, 3221 (1995).
B. Farid, in Electron Correlation in the Solid State, Ed. N. H. March, World Scientific/Imperial College Press 1999.
W. G. Aulbur, L. Jönsson, and J. W. Wilkins, Solid State Phys. **54**, 1 (1999).
L. Hedin, J. Phys.: Condens. Matter **11**, R489 (1999).
[8] O. Pulci, G. Onida, R. Del Sole, and L. Reining, Phys. Rev. Lett. **81**, 5374 (1998).
[9] N. Esser, N. Hunger, J. Rumberg, W. Richter, R. Del Sole, and A. I. Shkrebtii, Surf. Sci. **307/309**, 1045 (1994).
[10] W. Hanke and L. J. Sham, Phys. Rev. B **12**, 4501 (1975);
Phys. Rev. B **21**, 4656 (1980).
[11] P. Lautenschlager, M. Garriga, L. Vina, and M. Cardona, Phys. Rev. B **36**, 4821 (1987).
[12] G. Onida, L. Reining, and A. Rubio, to appear in Rev. Mod. Phys. (2002).
[13] F. Bechstedt, W. G. Schmidt, and P. Hahn, phys. stat. sol. (a) **188**, 1383 (2001) (this issue).
[14] G. Onida, L. Reining, R. W. Godby, R. Del Sole, and W. Andreoni, Phys. Rev. Lett. **75**, 818 (1995).
[15] M. Rohlfing and S. G. Louie, Phys. Rev. Lett. **83**, 856 (1999).
[16] M. Rohlfing, M. Palummo, G. Onida, and R. Del Sole, Phys. Rev. Lett. **85**, 5440 (2000).

[17] H. HIRAYAMA, N. SUGIHARA, and K. TAKANAYAGI, Phys. Rev. B **62**, 6900 (2000).
[18] R. M. FEENSTRA, G. MEYER, F. MORESCO, and K.H. RIEDER, Phys. Rev. B **64**, 081306 (2001).
[19] S. NANNARONE, P. CHIARADIA, F. CICCACCI, R. MEMEO, P. SASSAROLI, S. SELCI, and G. CHIAROTTI, Solid State Commun. **33**, 593 (1980).
[20] W. G. SCHMIDT, F. BECHSTEDT, K. FLEISCHER, C. COBET, N. ESSER, W. RICHTER, J. BERNHOLC, and G. ONIDA, phys. stat. sol. (a) **188**, (2001) (this issue).
[21] M. PALUMMO, G. ONIDA, R. DEL SOLE, and B. MENDOZA, Phys. Rev. B **60**, 2522 (1999).
[22] W. G. SCHMIDT, F. BECHSTEDT, and J. BERNHOLC, Phys. Rev. B **63**, 5322 (2001).
[23] W. LU, W. G. SCHMIDT, E. L. BRIGGS, and J. BERNHOLC, Phys. Rev. Lett. **85**, 4381 (2000).
[24] D. PAGET, private communication (2001).
[25] O. PULCI, B. ADOLPH, U. GROSSNER, and F. BECHSTEDT, Phys. Rev. B **58**, 4721 (1998).
O. PULCI, B. ADOLPH, and F. BECHSTEDT, phys. stat. sol. (a) **170**, 423 (1998).
[26] R. DEL SOLE and G. ONIDA, Phys. Rev. B **60**, 5523 (1999).
[27] E. D. PALIK, Handbook of Optical Constants of Solids, Academic Press, New York 1985.
[28] A. MARINI, R. DEL SOLE, and G. ONIDA, Phys. Rev. B **64**, 195125 (2001).
[29] S. GOEDECKER, Comput. Phys. Commun. **76**, 294 (1993);
SIAM J. Sci. Comput. **18**, 1605 (1997).